Biochemical Engineering Journal 99 (2015) 61–66

Contents lists available at ScienceDirect

Biochemical Engineering Journal

journal homepage: www.elsevier.com/locate/bej

Short communication

A hydrodynamic description of the flow behavior in shaken flasks

E. Mancilla[a], C.A. Palacios-Morales[a], M.S. Córdova-Aguilar[a], M.A. Trujillo-Roldán[b], G. Ascanio[a,*], R. Zenit[c]

[a] Centro de Ciencias Aplicadas y Desarrollo Tecnológico, Universidad Nacional Autónoma de México, Circuito Exterior, Ciudad Universitaria, Distrito Federal 04510, Mexico
[b] Instituto de Investigaciones Biomédicas, Universidad Nacional Autónoma de México, C.U., Distrito Federal 04510, Mexico
[c] Instituto de Investigaciones en Materiales, Universidad Nacional Autónoma de México, Distrito Federal 04510, Mexico

ARTICLE INFO

Article history:
Received 1 September 2014
Received in revised form 27 February 2015
Accepted 4 March 2015
Available online 10 March 2015

Keywords:
Bioreactors
Fluid mechanics
Mixing
Newtonian fluids
Hydromechanical stresses

ABSTRACT

Shaking flasks bioreactors have been employed extensively in biotechnology research for a long time. Despite of their wide application and importance, there is still insufficient knowledge about the hydrodynamic factors that determine the correct performance of growing cultures. The objective of this work is to provide a hydrodynamic description of the parameters which control the effective performance of such bioprocesses. The flow behavior of shaken flasks was examined using the particle image velocimetry technique (PIV) to capture the mixing dynamics for a range of operating conditions. The velocity fields and turbulent intensities were obtained. For all cases, the chaotic-like fluid motion increased with the orbital speed of the shaker. The behavior of conventional, coiled and baffled flasks was analyzed for shaking speeds ranging from 25 to 250 rpm; at high shaking rates the turbulent distribution increased for each flask configuration but the average value differed significantly. The highest turbulent intensity was found for the one-baffle arrangement, which is about 25% larger than the other configurations. We found that the highest turbulent production for all the different geometric conditions occurred at a shaking speed of about 150 rpm, which is in good agreement with the findings reported for the production of bacterial cultures at such shaking rate.

1. Introduction

Since the beginning of the century, shaking reactors have been used in many biotechnological processes [1,2]. For many years shaken flasks have been implemented in microbial fermentation, bacterial growth and in the pharmaceutical industry, among others [3–5]. The extensive use of shaken flasks relies on its simplicity, low cost and easy operation. In the biochemical industry the selection of the first step of a production process is very important prior to the scaling up to industrial scales. For this reason the characterization and determination of the appropriate operating conditions play a significant role in every process. Despite the importance of this initial step, only few investigations have attempted to understand the hydrodynamic foundations of orbital shakers. Büchs et al. [6–8], were the first authors to identify the hydrodynamic condition that restricts the operating performance in such systems. They reported a range of operation conditions. The regime called "out-of-phase" shaking, is distinguished by an augmentation of the fluid not following the orbital motion of the flask walls. In this case the specific power consumption is minimal, reducing the mass transfer rate and the mixing times. For this reason, in order to obtain a correct performance in such systems this behavior must be avoided. In shaking flask operations, multiple variables exist and have to be taken into account to describe the agitated system. Some of these parameters are the vessel geometry, size and orientation of the baffles, the liquid volume and operating conditions such as shaking radius and frequency, just to name a few. The conventional experiments performed in shaken flasks contribute to the knowledge of the operational conditions necessary to achieve the correct degree of mixing or the oxygen quantity needed in biochemical reactions. The main parameter considered in most studies is the rotational speed, which itself does not quantify other important engineering parameters as the oxygen mass transfer [9,10], the specific power consumption [11,12] or the hydromechanical stress [13–15] for which some cultures growing could be affected. For many years these parameters were inferred through large scale experiments or by the use of empirical correlations. But there are still large disagreements about the use of the physical variables that describe the hydrodynamic state in such bioreactors.

* Corresponding author.
E-mail addresses: gabriel.ascanio@ccadet.unam.mx (G. Ascanio), zenit@unam.mx (R. Zenit).

http://dx.doi.org/10.1016/j.bej.2015.03.003
1369-703X/

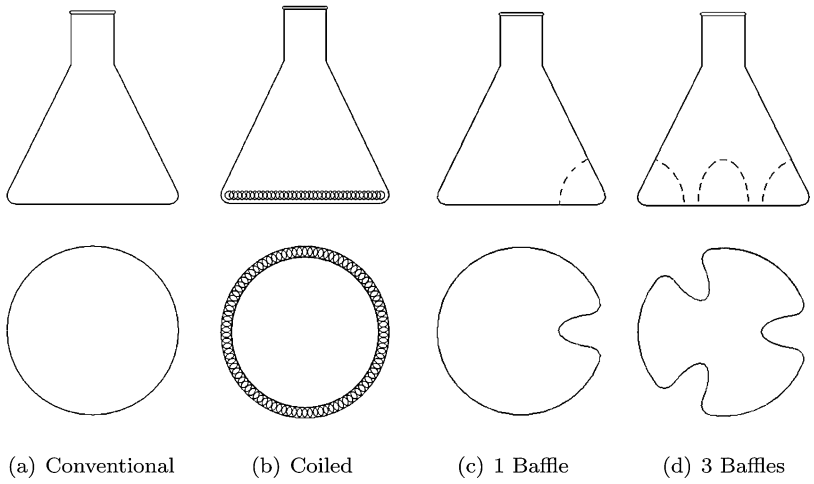

Fig. 1. Shaken flask configurations. The 2 and 4-baffles configurations are not shown.

As mentioned before, the specific power consumption has been used as key parameter for scaling up of growing culture processes [16]. Besides the power drawn, the influence of the flask geometry on the hydrodynamic performance should be also considered for scaling up purposes. Results from this study may help to select the appropriate impeller geometry by providing large turbulent intensities with the aim of enhancing mixing while shortening mixing times.

For such a purpose and in order to accomplish a better understanding of the internal process, it is necessary to analyze the flow fields and the spatial distribution of the turbulent intensity. The goal of this study is to get a deeper insight of the mixing behavior of shaken flasks as a function of their geometry with the aim of elucidating its performance from the standpoint of basic physical phenomena. Note that in this study, the effect of flow on growing cell culture was not assessed. We focused only on the hydrodynamic state of shaken flasks and how better mixing can be achieved with different configurations and shaking speeds.

2. Materials and methods

2.1. Experimental setup

Six different configurations of 250 ml Erlenmeyer flasks (Pyrex,Mexico) with 82 mm of maximum diameter were tested: conventional, baffled and coiled as shown in Fig. 1. Similar flask configurations were used by Gamboa-Suasnavart et al. [17]. The conventional flasks have a standard design which consists of a round circular section. Baffled flasks had a different number of baffles and indentations (1, 2, 3 and 4) placed at equidistant sections with 20 mm depth and 45 mm height. The coiled configuration consists of conventional flask into which a 30 cm stainless steel spring (1.3 cm diameter, 19 SW) is inserted. To have similar fluid characteristics, each flask was filled with 50 ml of Luria-Bertani's medium and a solution of 34% (w/v) sucrose was added. The liquid depth (from bottom to liquid surface) was 10 ± 2 mm depending on the flask configuration. The fluid had the following properties: $\rho = 1300\ kg/m^3$, $\mu = 3.5$ mPa·s and $\sigma = 62$ mN/m (surface tension). The flasks were agitated in an orbital standard shaker (VWR, model Signature DS 500), with a counterbalanced eccentric drive mechanism that travels over a 19 mm circular orbit (shaking diameter) for a speed range from 50 to 200 rpm (shaking frequency).

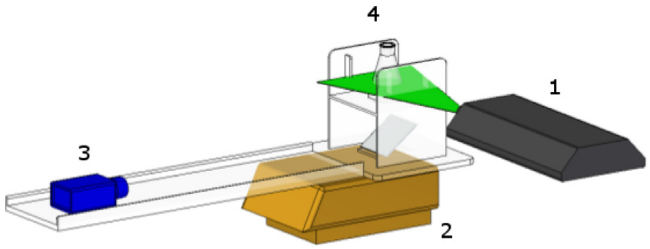

Fig. 2. Experimental setup: The laser (1), orbital shaking device (2), camera (3) and the flask array (4) are depicted.

2.2. Velocity field measurements

Fig. 2 shows the experimental setup used for determining the flow fields using the particle image velocimetry technique (PIV). It consisted of a pulsed laser light (Solo III HiSense Dynamics, wavelength of 532 nm, energy of 150 mJ), an optical array for creating a light sheet of 2 mm width and a CCD camera (Kodak Megaplus, Model ES 1.0) and a 35 mm lens, both placed in front of a mirror, inclined 45 degrees. The flask was placed into a square jacket containing water for minimizing the optical distortion due to the flask curvature. The laser sheet was aligned parallel to the base of the flask and with a height of 5 mm from the bottom; i.e. in the middle of the total depth. Note that in our measurements the camera was mounted on the same shaking plate where the flask was placed: the fluid velocity was obtained in the reference frame of the flask. For this study, an acquisition rate of 4 Hz was chosen. The Flow Manager software (Dantec Dynamics) was used to control the system and to process the images. The time between image pairs was varied from 1000 μs to 2500 μs, depending on the velocity of the orbital plate. Sets of 300 images were captured for each experiment in order to ensure a statistically robust average. The incorporation of air bubbles during the shaking caused unwanted laser reflections, which were filtered out using fluorescent particles (10 μm, Dantec Dynamics) and a 550 nm optical filter (mounted on the camera lens). The velocity fields were inferred using the standard cross correlation method used in PIV, considering interrogation areas of 32×32 square pixels area (about 1.6 mm^2) with an overlap of 50×50%. A spatial filter (3×3 pixels) was applied to eliminate spurious vectors. The velocity fields were obtained from the statistical average of the images. The velocity magnitude and turbulence intensity were inferred from the time averaged velocity fields.

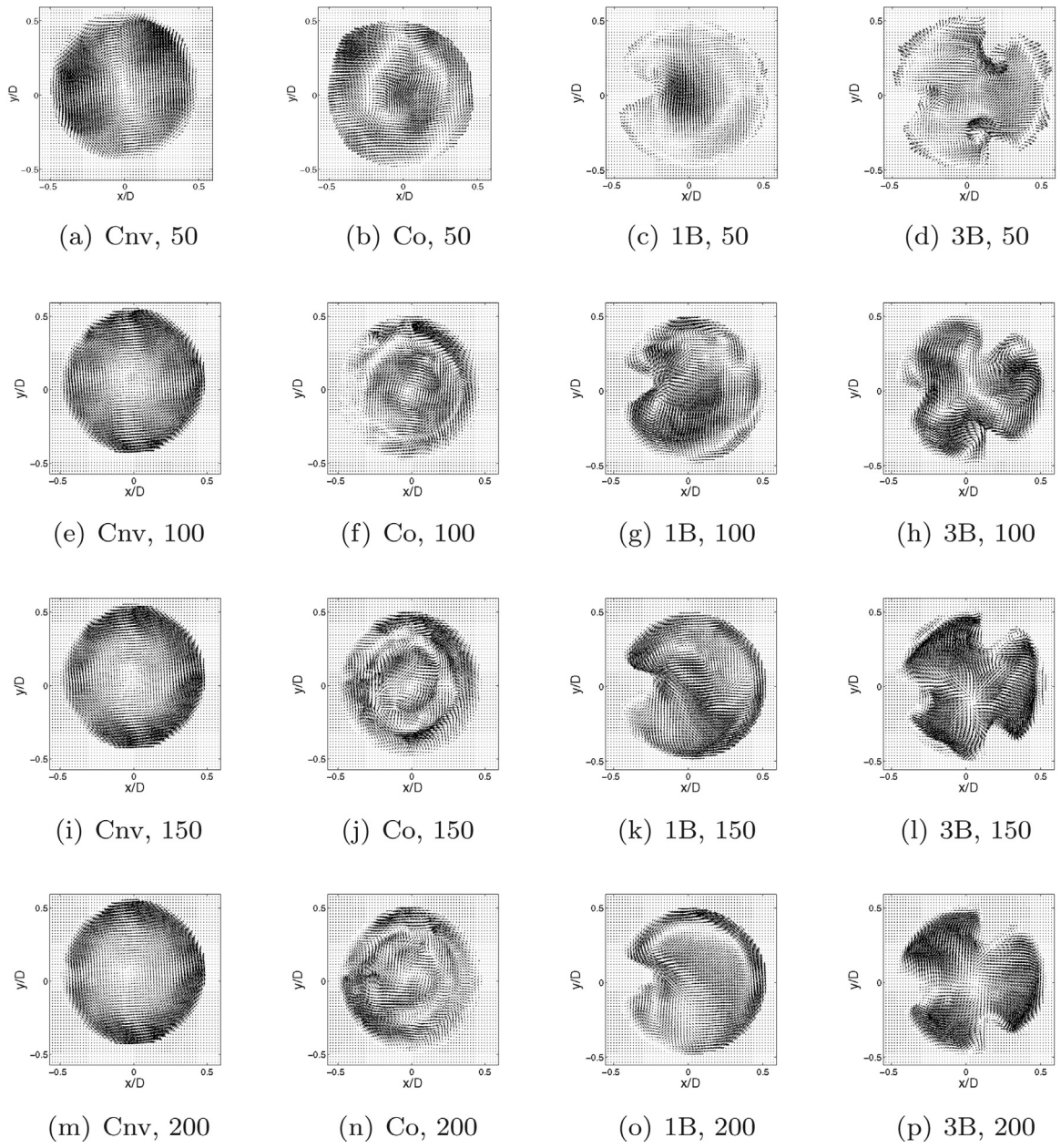

Fig. 3. Average flow patterns for the Conventional (Cnv), Coiled (Co), 1-Baffle (1B) and 3-Baffles (3B) flasks at different orbital velocities. The numbers denote the different orbital velocities in rpm.

The magnitude of the velocity was estimated as:

$$U = \sqrt{u^2 + v^2} \tag{1}$$

where u and v are the velocity components in the x and y directions, respectively. The turbulent intensity was calculated from the velocity fluctuations:

$$IT = \frac{\sqrt{u'^2 + v'^2}}{U_l} \tag{2}$$

where u' and v' are the fluctuating velocities at each direction of the flow field (calculated from the standard deviation of the velocity in different times) and $U_l = D_f\ \omega$ is the shaking velocity of the device, where D_f is the flask diameter and ω is the rotational speed in rps.

We use the turbulent intensity as a measure of the fluid agitation. The agitation is simply the variability of the velocity in a given flow; this quantity is greatly influences the transfer rates of heat and mass [18].

3. Results

The flow inside the shaken flask was investigated experimentally and an analysis of their distinctive features is presented here. Firstly, the flow patterns generated in each geometrical configuration is presented. In the second section, the calculated turbulent intensity fields are shown. which were inferred from the time average of the velocity fields.

3.1. Velocity fields

In Fig. 3, we show the averaged velocity fields at different orbital speeds. The shaking motion was counter-clockwise for all cases. As expected, the motion of the liquid for the various recipient

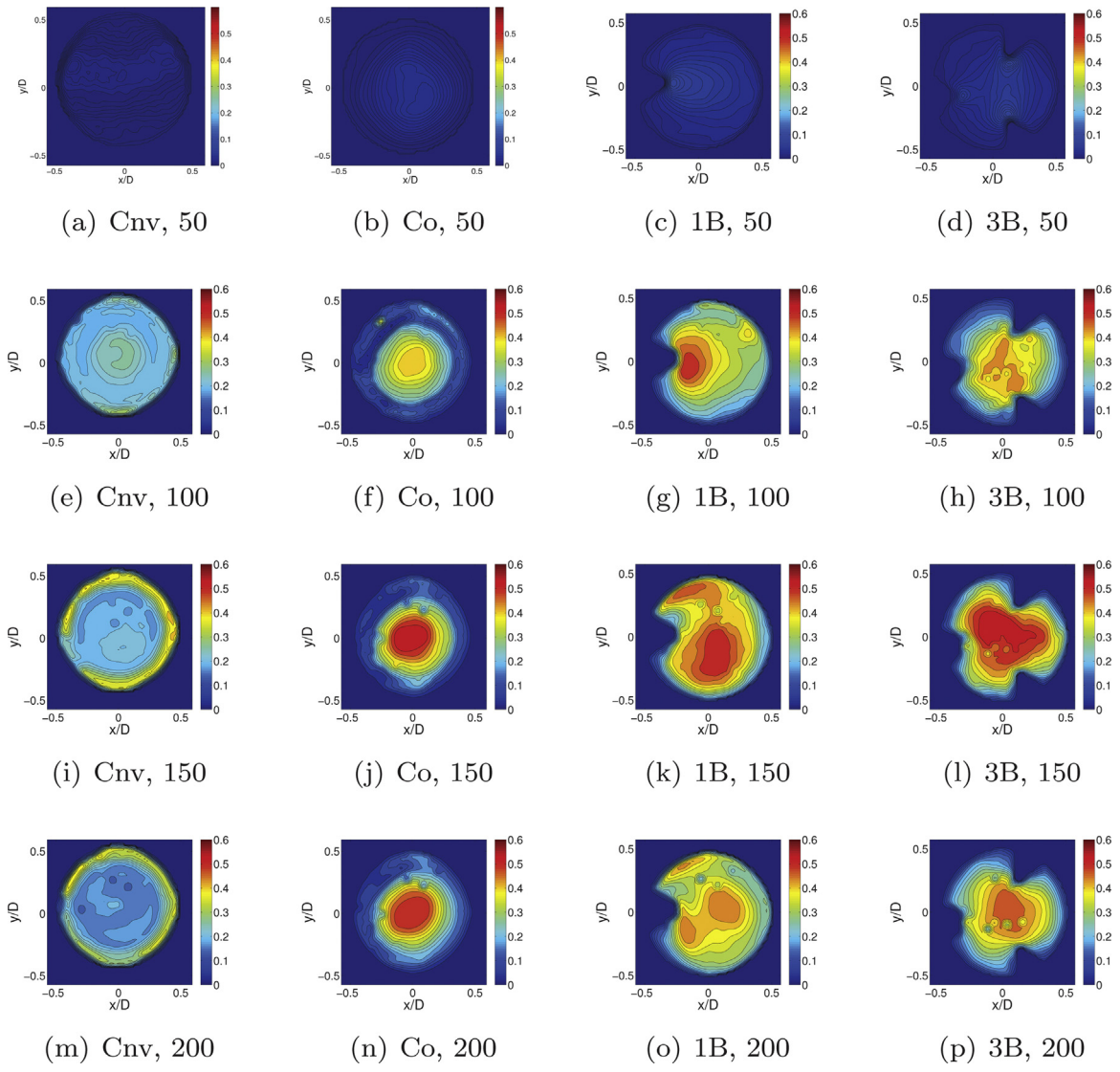

Fig. 4. Turbulent intensity fields for the Conventional (Cnv), Coiled (Co), 1-Baffle (1B) and 3-Baffles (3B) flasks at different orbital velocities. The numbers denote the different orbital velocities in rpm. The colors denote the magnitude of turbulent intensity: warm (reps. cool) colors denote high (reps. low) values of turbulent intensity. For clarity, all the maps have the same scale. (For interpretation of the references to color in this figure legend, the reader is referred to the web version of the article.)

configurations is different for each case; evidently, the flow behavior depends on the flask geometry and the shaking speed. The velocity fields for the conventional flask, shown in Fig. 3(a, e, i and m), did not change significantly with the shaking speed. The liquid tended to accumulate near the flask walls in the shaking direction, forming a circular solid-body-like movement with small regions of high velocity close to the wall. For all the shaking velocities the conventional flask showed a small interaction of fluid at the center of the flask resulting in poor mixing. For the coiled flask, shown in Fig. 3(b, f, j and n), we observed similar differences in the liquid behavior for all shaking speed range, i.e. the velocity patterns remained nearly constant and strong circulations were not observed. In particular, for this case, two zones of separated flow were identified; one of them was clearly located in the center of the flask in which there was no interaction with the surrounding flow and the second region near the wall where the flow interacted with the coil. In this second region, as the velocity increased, mixing between the inner and outer zones started, but no significant mixing in the bulk was presented.

Significant changes in flow behavior were observed as the shaking speed was increased for the baffled flask configurations, Fig. 3 (c, g, k and o) and (d, h, l and p). At low agitation speed (50 rpm), a small flow was created in the surroundings and most of the flow was concentrated at the center of the vessel. The formation of small vortices in regions close to the baffles was observed due to the interaction of the main stream with each of the indentations (see Fig. 3(c) and (d)). For the baffled flasks, significant changes in flow configuration were observed as the shaking speed increased. When the speed increased to 100 rpm a large vortex appears. A coherent flow structure is identified, formed by vortices of different sizes (Figs. 3(g) and (h)). We identified low intensity vortices located near the flask walls and larger vortices formed in the front and rear part of each deflector. At this operating condition the fluid was mixed in the walls but in the center of the container, no significant streams were observed. When the shaking speed was increased to 150 rpm, which is similar to the agitation velocity at which microorganisms cultures are produced [17,19,20], the liquid moved in the shaking direction close to the walls, which consequently produced significant fluid streams. As shown in Fig. 3(k) and (l), such streams interacted with the geometry, particularly with the flask baffles. This allowed for distribution of the stream which occupied most of the vessel and caused the formation of vortices inducing the mixing

of the various fluid layers. For the other configurations, the fluid and baffles interaction disrupted the mean flow and generated a significantly asymmetrical flow that promoted the appearance of secondary recirculation zones and induced mixing. As mentioned before, the behavior at this shaking rate was different for the single and the other baffled flasks, but all of them generated a more homogeneous velocity distribution and the maximum velocities were located just in the front side and rear side of each indentation. We could also note that the central mixing region was larger than that at lower agitation speeds. For the case of 200 rpm all the baffled flasks showed a similar performance, in which most of the flow and higher speeds were in the area close to the walls but the main stream was colliding with the baffles at a slower velocity than at 150 rpm, as shown in Fig. 3(o) and (p).

3.2. Turbulent intensities

The different flow patterns significantly affect the turbulent intensity distribution inside the flasks. The average turbulent intensity contour maps for the different configurations are shown in Fig. 4 for a range of shaking rates (from 50 to 200 rpm). Note that these maps correspond to the velocity fields shown in Fig. 3. In all cases, high zones of fluctuating velocities were found near the obstacles, namely coil or baffles. In general, the turbulence intensity increases with the shaking speed for all cases as expected. For the conventional flask, we observe that the largest turbulence intensity is located at the periphery of the flask, i.e. at the vicinity of the walls Fig. 4(a, e, i and m). The turbulence intensity at the center of the flask is homogenous but relatively low. This means that the fluctuations occur mainly at the flask walls, which is not the ideal condition because the mixing (mass transfer) at the center of the flask is poor. For the coiled configuration, the distribution of turbulence intensities improved slightly without showing a noticeable interaction with the coil, as shown in Fig. 4(b,f, j and n). A small increase in the turbulence intensity with respect to the previous case can be noted. It is important to note that the turbulence intensity inside the metallic spring is relatively small; the coil dampens velocity fluctuations. In any case the mixing between the coil region and the flask center is not greatly improved. In particular for this case, we observe two regions of flow: inside and outside the coil. For the one-baffle flask, the turbulent intensity is distributed uniformly, as depicted in Fig. 4(c, g, k and o). In this case, an increase of the turbulent intensity level is observed, reaching a maximum value at around 150 rpm. When the orbital speed was increased beyond this value, the turbulent intensity level did not increase; in fact, a small reduction was identified.

For the three-baffle configuration, shown in Fig. 4 (d, h, l and p), also an increase of the magnitude and homogeneity of the turbulent intensity field were observed. The maximum was reached at around 150 rpm. Note that the two and four baffle configurations (not shown) showed similar behavior. However, the magnitude of turbulent intensity was smaller than the one generated for the one-baffle flask. It is remarkable to note that a homogeneous turbulent distribution was accomplished when increasing shaking rates for all the systems described here. Beyond this threshold value of 150 rpm, the shaking speed did not cause an increase of the turbulent intensity average value. This finding is in agreement with previous reports [17,20]. The velocity fluctuations generated in each of the indentations interacted with the flow fluctuation generated in the next baffle, promoting their rapid dissipation. The presence of obstacles within the flasks, whether coils or baffles, cause large velocity fluctuations improving the mixing process. In particular, for the baffled configurations, the turbulence intensity is more homogenous along the entire flow area, which means that different layers of the flow are well mixed, promoting in consequence efficient mass transfer.

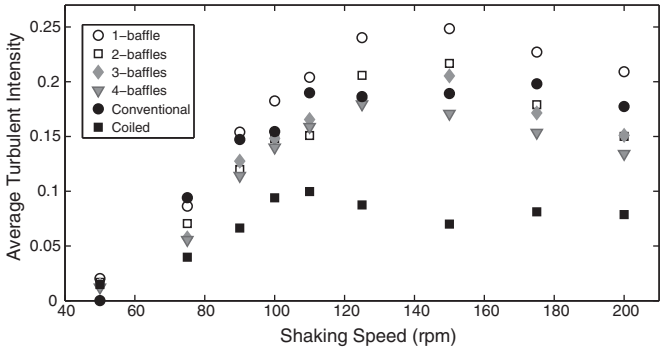

Fig. 5. The average turbulent intensity for each flask as a function of the shaking rate.

The overall performance of shaking flasks can be presented in a concise manner plotting the mean turbulent intensity, for each condition, as a function of the shaking speed. This plot is presented in Fig. 5. Clearly, achieved for a given flask depends on both the shaking speed and flask geometry. In all cases, a maximum level of turbulent intensity is achieved at around 150 rpm. The level of agitation intensity depends on the number of baffles. Baffles are needed to deflect the flow and induce the interaction of the induced streams. However, too many baffles do not improve the level of agitation. As observed in the velocity fields, the induced currents may 'cancel' each other reducing circulation and limiting the amount of mixing.

4. Conclusions

Shaken flasks have been extensively used in the development of biotechnological processes. It is known that the flow in such systems plays a significant role in the quality of the final products. Thus, the basic understanding of the hydrodynamic state is necessary to optimize such processes. The physical parameters to be taken into account are the hydromechanical stresses, mainly influenced by the turbulent intensity. A hydrodynamic analysis for agitated flasks was carried out using six different geometrical configurations and a range of shaking velocities. From examined data, it is clear that the hydrodynamic behavior is directly related to the shaking velocity and the geometry of the flask. It was noted that the flow fields produced by the flasks baffles or coils exert a considerable influence on the hydrodynamic features across the whole vessel. The turbulent intensity can be used to determine the quality of the agitation since cultures are sensitive to these parameters. For that reason, it is important to pay special attention to the maximum values of this parameter for specific operations. It must be noted, however, that a more complete hydrodynamic characterization of this system could be achieved by also considering the amount of shear in the induced flow. An increase of the shaking rate results in higher shear stresses, which can be a drawback, particularly when working with shear sensitive media such as a cell cultures [15]. The shear rate can be quantified directly from the velocity field measurements [18].

The analysis of the flow fields showed that the highest velocity gradients are located near the baffle indentations. The 150 rpm orbital velocity was identified as a critical shaking speed to achieve more homogeneous turbulent distribution and a maximum value for most of the flask configurations tested in this investigation. It was observed that over passing this limit the turbulence values diminish considerably. We can conclude that the baffled flasks have a nearly homogeneous turbulent distribution with large intensity values in comparison with the coiled flask. Although in previous works similar agitation rate or power input was used

between conventional, coiled and baffled flasks different physiological responses were observed in filamentous recombinant bacterial cultures [17,20], surely due to homogeneous distribution of the turbulent intensity. In particular, the one-baffle configuration showed better hydrodynamic performance. In general, we can conclude that baffled flasks could be a good option for microscopic organism, bacteria, virus, or fungus cultivation. In addition to mixing, the agitation needs to be of moderate mechanical stress, since they both determine the quantity and quality of production, and some microorganisms are sensitive to the latter. This study provides the first attempt to relate the hydrodynamic performance with the cultures production and morphology control. Note that this study only considered one size of flasks. To further improve our understanding of fluid mixing and, most importantly, the scaling of these systems, more experiments would have to be conducted considering different vessel sizes and possibly other liquids. Another aspect that also needs to be addressed in future studies is the effect of biocultures. Once organisms start to grow within the shaken flasks, the properties of the fluid may be affected and, as a result, the level of agitation may change. We plan to study these ideas in the future.

Acknowledgements

The financial support from DGAPA-UNAM through the grant IN-108312 is highly appreciated. We also thank Miguel Bazán for the technical support.

References

[1] D. Freedman, The shaker in bioengineering, Methods Microbiol. 2 (1970) 175–185.
[2] S. Suresh, V. Srivastava, I. Mishra, Critical analysis of engineering aspects of shaken flask bioreactors, Crit. Rev. Biotechnol. 29 (4) (2009) 255–278.
[3] C.-M. Liu, L.-N. Hong, Development of a shaking bioreactor system for animal cell cultures, Biochem. Eng. J. 7 (2) (2001) 121–125, Special issue: Shaking Bioreactors.
[4] J. Büchs, Introduction to advantages and problems of shaken cultures, Biochem. Eng. J. 7 (2) (2001) 91–98.
[5] T. Anderlei, C. Cesana, C. Burki, M. De Jesus, M. Kuhner, F. Wurm, R. Lohser, Shaken bioreactors provide culture alternative, Genet. Eng. News 29 (2009) 19.
[6] C.P. Peter, Y. Suzuki, K. Rachinskiy, S. Lotter, J. Büchs, Volumetric power consumption in baffled shake flasks, Chem. Eng. Sci. 61 (11) (2006) 3771–3779.
[7] J. Büchs, S. Lotter, C. Milbradt, Out-of-phase operating conditions, a hitherto unknown phenomenon in shaking bioreactors, Biochem. Eng. J. 7 (2) (2001) 135–141.
[8] J. Büchs, U. Maier, C. Milbradt, B. Zoels, Power consumption in shaking flasks on rotary shaking machines: II. Nondimensional description of specific power consumption and flow regimes in unbaffled flasks at elevated liquid viscosity, Biotechnol. Bioeng. 68 (6) (2000) 594–601.
[9] T. Anderlei, J. Büchs, Device for sterile online measurement of the oxygen transfer rate in shaking flasks, Biochem. Eng. J. 7 (2) (2001) 157–162.
[10] T. Anderlei, W. Zang, M. Papaspyrou, J. Büchs, Online respiration activity measurement (otr, ctr, rq) in shake flasks, Biochem. Eng. J. 17 (3) (2004) 187–194.
[11] Y. Kato, S. Hiraoka, Y. Tada, S. Koh, Y. Lee, Mixing time and power consumption for a liquid in a vertical cylindrical vessel, shaken in a horizontal circle, Chem. Eng. Res. Des. 74 (4) (1996) 451–455.
[12] Y. Sumino, H. Fukuda, S. Akiyama, Performance of shaking flask. 1. Power consumption, J. Ferm. Bioeng. 50 (3) (1972) 203.
[13] C.P. Peter, Y. Suzuki, J. Büchs, Hydromechanical stress in shake flasks: correlation for the maximum local energy dissipation rate, Biotechnol. Bioeng. 93 (6) (2006) 1164–1176.
[14] M. Fujita, K. Iwahori, S. Tatsuta, K. Yamakawa, Analysis of pellet formation of *Aspergillus niger* based on shear stress, J. Ferm. Bioeng. 78 (5) (1994) 368–373.
[15] M.A. Trujillo-Roldán, N.A. Valdez-Cruz, El estrés hidrodinámico: Muerte y daño celular en cultivos agitados, Rev. Latinoam. Microbiol. 48 (3) (2006) 269–280.
[16] G. Rodriguez, T. Anderlei, M. Micheletti, M. Yianneskis, A. Ducci, On the measurement and scaling of mixing time in orbitally shaken bioreactors, Biochem. Eng. J. 82 (0) (2014) 10–21.
[17] R.A. Gamboa-Suasnavart, N.A. Valdéz-Cruz, L.E. Cordova-Dávalos, J.A. Martínez-Sotelo, L. Servín-González, C. Espitia, M.A. Trujillo-Roldán, The o-mannosylation and production of recombinant apa (45/47 kda) protein from mycobacterium tuberculosis in *Streptomyces lividans* is affected by culture conditions in shake flasks, Microb. Cell Fact. 10 (2011) 110–120.
[18] P. Kundu, I. Cohen, Fluid Mechanics, Elsevier, New York, 2000, 76 pp.
[19] R. Gamboa-Suasnavart, L. Marín-Palacio, J. Martínez-Sotelo, C. Espitia, L. Servín-González, N. Valdez-Cruz, M. Trujillo-Roldán, Scale-up from shake flasks to bioreactor, based on power input and *Streptomyces lividans* morphology, for the production of recombinant apa (45/47 kda protein) from *Mycobacterium tuberculosis*, World J. Microbiol. Biotechnol. 29 (2013) 1421–1429.
[20] L. Marín-Palacio, R. Gamboa-Suasnavart, N. Valdez-Cruz, L. Servín-González, M. Córdova-Aguilar, E. Soto, W. Klöckner, J. Büchs, M. Trujillo-Roldán, The role of volumetric power input in the growth, morphology, and production of a recombinant glycoprotein by *Streptomyces lividans* in shake flasks, Biochem. Eng. J. 90 (2014) 224–233.